Green Chemistry

PAPER

View Article Online
View Journal | View Issue

Check for updates

Cite this: *Green Chem.*, 2021, **23**, 4386

Energy and techno-economic analysis of bio-based carboxylic acid recovery by adsorption†

Patrick O. Saboe, Lorenz P. Manker,‡ Hanna R. Monroe, William E. Michener, Stefan Haugen, Eric C. D. Tan, Ryan L. Prestangen, Gregg T. Beckham and Eric M. Karp *

Received 22nd March 2021,
Accepted 2nd June 2021

DOI: 10.1039/d1gc01002f

rsc.li/greenchem

Recent works have established bio-based carboxylic acids as adaptable precursors to renewable biofuels and chemicals. However, the separation of carboxylic acids is a major energy and cost driver, accounting for 20–40% of the entire processing cost. Improved downstream separation technologies that reduce operating costs compared to conventional approaches are needed, particularly to enable bio-based commodity fuels and chemicals. Here, we combine techno-economic analysis (TEA) and an energy and environmental assessment with experimental results to compare weak-base adsorption (WBA) processes with the conventional strong ion exchange (IX) process for the recovery of the exemplary product, butyric acid. TEA indicates that WBA has the potential to reduce operating expenses from 34% to 6% relative to the selling price of butyric acid ($1.8 kg^{-1}). Our energy analysis shows that the WBA process has 12.2-fold energy reduction and 9.2-fold GHG emission reduction compared to the conventional IX process.

1. Introduction

The production of bio-based chemicals and fuels is a compelling pathway for next generation products that offer sustainable manufacturing and a more circular carbon economy.[1] In particular, the microbial production of bio-based carboxylic acids from both monocultures[2] and mixed cultures[3] is an attractive technology option that benefits from a high conversion selectivity from complex and sustainable feedstocks such as lignocellulosic biomass,[4] food waste,[5] and syngas.[6] Following microbial production, carboxylic acids are versatile intermediate with available chemistry for conversion to many commodity and specialty chemicals including liquid fuels,[7–9] polymer precursors,[10,11] food additives,[12] and pharmaceuticals.[13] However, a major challenge in the production of bio-based chemicals derived from carboxylic acids is the required bioseparations which typically account for 20–40% of the total production cost.[14]

Reducing the energy demand of carboxylic acid recovery is critical to achieve cost competitive bio-based chemicals. Techno-economic analysis (TEA) shows that the cost of a biorefinery correlates directly (R^2 = 0.88) to the plant energy efficiency, with separations contributing the largest proportion of the total energy consumption.[15] One of the most energy intensive steps in bioseparations is the removal of water from the product stream, which is traditionally completed using thermal driven technologies such as distillation because it is a mature technology. As most bioprocesses produce carboxylic acids in dilute aqueous streams (<15 wt%), water removal *via* distillation and evaporation is a major contributor to the overall energy demand of the separation train.[2,16] Furthermore, short-chain carboxylic acids (SCCAs) such as acetic acid or butyric acid have azeotropes with water, causing the distillation process to be highly energy intensive.[17,18] To that end, alternative technologies are emerging for carboxylic acid recovery, such as liquid–liquid extraction,[19] nanofiltration,[20] and adsorption.[21] Among these approaches, adsorption is a leading technology option to separate bio-based products that offers several key advantages including a high selectivity for carboxylic acids and scalable systems.[22–24]

The most common approach in adsorption technologies for bio-based carboxylic acid is to employ a highly selective strong ion exchange (IX) resin which ionically binds the product carboxylic acid, enabling the removal of contaminants such as sugars from the product stream (Table S1†). However, the use of a strong IX resin requires concentrated acid and/or base to desorb the bound carboxylate, acidify the carboxylate, and to regenerate the resin,[24] thereby adding a considerable raw material cost to the process.[25] To minimize raw material cost,

Renewable Resources and Enabling Sciences Center, National Renewable Energy Laboratory, Golden, CO, USA. E-mail: eric.karp@nrel.gov

†Electronic supplementary information (ESI) available. See DOI: 10.1039/d1gc01002f

‡Current address: Laboratory of Sustainable and Catalytic Processing (LPDC), Institute of Chemicals Sciences and Engineering (ISIC), School of Basic Sciences (SB), Ecole Polytechnique Fédérale de Lausanne (EPFL), 1015 Lausanne, Switzerland.

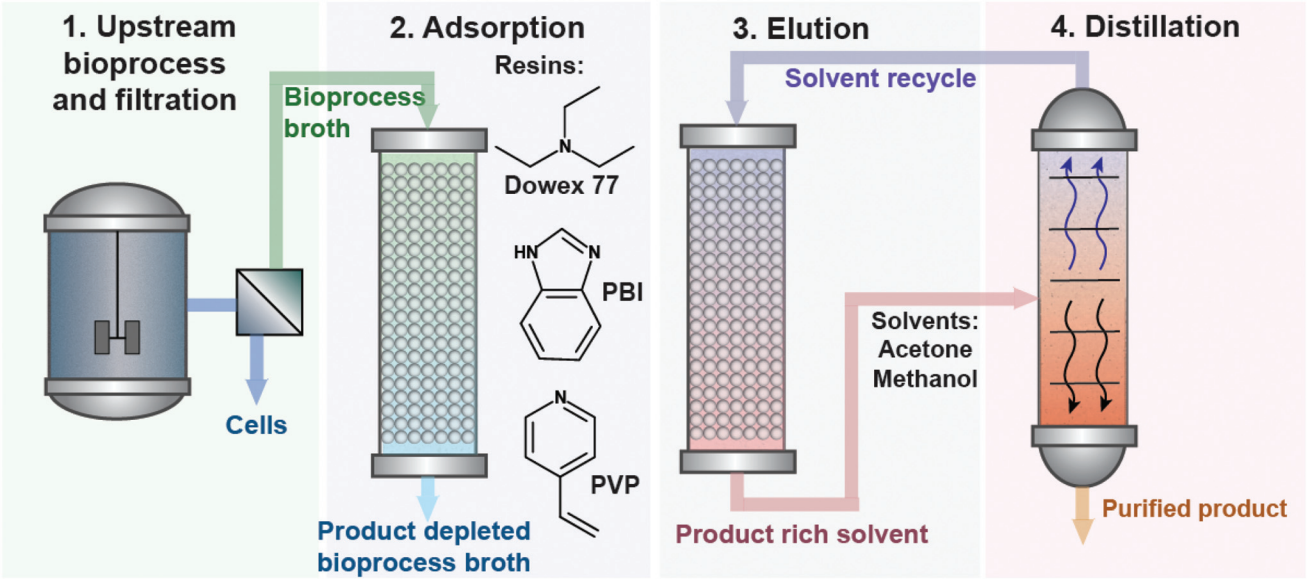

Fig. 1 WBA process flow diagram. (1) The bioprocess broth containing a bio-based carboxylic acid is first filtered to remove microbes from the product stream. (2) The product carboxylic acid is adsorbed onto the nitrogen containing functional groups of a weak-base resin such as Dowex 77, PBI, or PVP. (3) The bound carboxylic acid is then eluted from the weak-base resin with a solvent such as acetone or methanol. (4) The elution solvent is then separated *via* distillation from the product carboxylic acid and recycled within the process.

industrial adsorption processes such as those developed for lactic and citric acid recovery utilize weak-base adsorption (WBA) technology in conjunction with thermal water evaporation methods.[22,26,27] As opposed to the strong IX process, a weak-base resin forms a reversible acid–base pairing between the resin and the acidic proton of the carboxylic acid.[28] This weak interaction is readily broken during elution with hot water, dilute acid or base, or an organic solvent such as methanol or acetone.[29] Organic solvents are an attractive alternative to aqueous elution because they can concentrate the carboxylic acid during elution, remove water non-thermally from the product stream, and are easily recycled by distillation (Fig. 1). While many weak-base resins including poly(4-vinylpyridine) (PVP),[30] tertiary amine resins,[31] and zeolites[32] have been characterized, design strategies for selecting a resin and elution system to minimize operating expenses (*i.e.* resin cost, solvent cost, energy cost) and the environmental impacts (*i.e.* greenhouse gas emissions and non-renewable energy consumption) is generally lacking. Furthermore, TEA and environmental impacts studies of WBA compared to conventional strong IX have not been reported to our knowledge.

To address the need for a systematic approach to optimize WBA technology for carboxylic acid recovery, economic feasibility and environmental impact, in this study, we correlate three process parameters including the (i) resin demand, (ii) energy demand, and (iii) elution solvent demand to two fundamental and readily available parameters (1) the pK_a of the resin and (2) the basicity of the elution solvent. The developed correlation enables selection of a resin and elution solvent pair to minimize the operating cost, energy demand, and environmental impacts without the need for extensive experimental data collection. To develop this correlation, we use a combination of experimental data from adsorption isotherms, fixed-bed column experiments, and Aspen Plus process modeling of distillation-based solvent recycling to quantify the required solvent, resin amount, and energy demand. We then provide comprehensive techno-economic analysis (TEA) and environmental impacts for several resin-elution solvent pairings. We selected butyric acid as the model carboxylic acid product because it is targeted as an intermediate for drop-in biofuel production[7] and can be produced from renewable feedstocks such as lignocellulosic biomass.[33] Lastly, we compare the TEA and environmental impacts of several weak-base adsorption processes to conventional strong ion exchange process.

2. Results

2.1. Equilibrium isotherms

We first adsorbed butyric acid onto weak-base resins to investigate the equilibrium behavior of the system which is useful towards estimating the amount of resin needed to adsorb a given amount of butyric acid. The adsorption capacity of three commercially available weak-base resins, poly(4-vinylpyridine) (PVP), poly(2,2′-*m*-phenylene-5,5′-dibenzimidazole) (PBI), and Dowex 77, which vary in their functional group (Table 1) was measured as a function of aqueous butyric acid concentration. The acid adsorption capacity (Fig. 2A) was determined over butyric acid concentrations in water within the range relevant to bioprocessing (generally less than 150 g L^{-1})[2] and is reported as the 'individual capacity', which accounts for the decrease in solution volume due to adsorption of acid and

Table 1 Resin information, Freundlich parameters, and resin pK_a value's

Resin name	Polymer backbone	Functional group	K	n^{-1}	Functional group pK_a	Apparent pK_a of resin
PVP	Poly(4-vinylpyridine)	Pyridine	0.049	0.59	5.23[34]	4.9[29]
PBI	Poly(2,2′-*m*-phenylene-5,5′-dibenzimidazole)	Benzimidazole	0.076	0.53	5.48[35]	5.3[29]
Dowex 77	Polystyrene-divinylbenze	Diethylbenzyl-amine	0.27	0.29	8.91[36]	7.6[29]

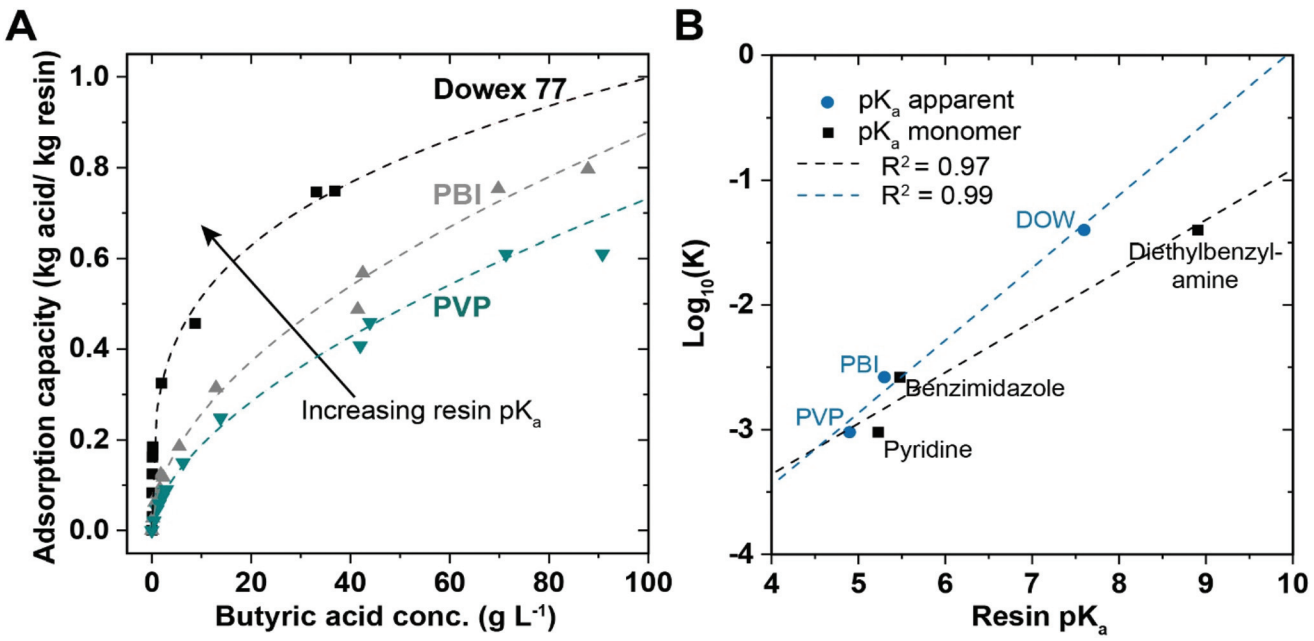

Fig. 2 Equilibrium isotherms. (A) The individual adsorption isotherms for butyric acid onto weak-base resins are shown, with dashed lines representing the fit from the Freundlich isotherm model (eqn (2)). (B) There is a linear correlation between the logarithm of the adsorption capacity and both the pK_a of the resins' functional group and the apparent pK_a of the resin (eqn (S2) and (S3)†).

water onto the resin. The individual capacity prevents the false calculation zero uptake when acid is adsorbed but no change in acid concentration is observed (this would occur if the resin adsorbed water and acid at the same ratio as they are present in the initial solution). Accordingly, eqn (1) was used to determine individual adsorption capacity data points in Fig. 2A:

$$q = \frac{V_o C_o - V_F C_{EQ}}{m_R}. \quad (1)$$

In eqn (1), q is the individual adsorption capacity of acid onto the resin (kg acid per kg dry resin), V_o is the initial volume of aqueous acid solution (L), C_o is the initial concentration of acid present in solution (g L^{-1}), V_F is the volume of liquid remaining in solution (L), C_{EQ} is the equilibrium concentration of acid remaining in the solution (g L^{-1}), and m_R (g) is the mass of dry resin added to the acid solution.

An equilibrium isotherm Freundlich model was then fit to adsorption data to estimate the amount of butyric acid per mass of resin as a function of the butyric acid concentration in the aqueous phase (indicated by the dotted lines in Fig. 2A). The Freundlich model is an empirical relationship that accounts for nonideal adsorption mechanisms, for example overloading of active sites (when two or more molecules are adsorbed on one active site)[37,38] and lateral interactions (when repulsive or cooperative effects are present).[38–40] The Freundlich model relates the concentration of acid on the resin to the concentration of acid in solution at equilibrium through the following equation:

$$q = K(C_{EQ})^{n^{-1}} \quad (2)$$

In eqn (2), q is the adsorption capacity of acid onto the resin (kg acid per kg dry resin), C_{EQ} is the equilibrium concentration of acid in the solution (g L^{-1}), K is the adsorption constant of the resin (L g^{-1}), and n^{-1} is a constant that indicates the linearity of the isotherm.

It is noteworthy that the butyric acid isotherms do not exhibit saturation (as would be indicated by an adsorption plateau). Thus, the Langmuir isotherm model (eqn (S1)†), which assumes ideal 1 : 1 molar interaction between adsorbent and active site leading to an adsorption plateau, does not provide a satisfactory description of butyric acid adsorption. The deviation from Langmuir isotherms may be due to nonideal adsorption mechanisms such as overloading or lateral interactions between adsorbed acid molecules.[40,41] The deter-

mined adsorption constant and *n*-values are listed in Table 1. Ultimately, these isotherm fits provide an estimate of the amount of resin needed to adsorb a given amount of butyric acid in the feed stream.

Since the selected resins differ in their functional group pK_a, an additional correlation relating the pK_a of the functional group to the adsorption constant was developed (Fig. 2B). To build this correlation the logarithm of the adsorption constant (K), which was determined from the Freundlich isotherm fits for each of the three resins in Fig. 2A, was plotted against the logarithm of the ionization constant (pK_a) of each resin's functional group. There are two ways to determine the pK_a of each resin used. The 'apparent' pK_a of the resin is determined by titrating the resin sample, and the 'monomer' pK_a is determined by titrating the free functional group monomer. In Fig. 2B, both the apparent pK_a and the monomer pK_a for each resin are plotted. A linear regression of the data points in Fig. 2B was performed to correlate the adsorption constant (K) of the resin to pK_a of the resin. The apparent pK_a appears to give a slightly better approximation based on the regression R^2 value (0.99 *vs.* 0.97) (eqn (S2) and (S3)†). The relationship shown is an example of the Linear Free Energy Relationship (LFER), where a known equilibrium constant (*i.e.* the acid dissociation constant (K_a)) is related to another equilibrium constant (*i.e.* the butyric acid adsorption constant (K)) by a linear double logarithmic function.[42] The LFER is relevant to many physical processes beyond adsorption including extraction to estimate the partitioning of small molecules into complex phases such as organic soil matter or skin.[43,44] Accordingly, we have developed correlation between the resin pK_a and the adsorption constant of butyric acid, which can be used to estimate the uptake of butyric acid based on simple pK_a measurements of the resin, which are readily available for many functional groups beyond the resin functional groups that we have investigated here. This methodology may be extrapolated to estimate the uptake of volatile fatty acids other than butyric acid based on the pK_a of the resin. Below, we show how the resin adsorption constant (K) influences desorption behavior, leading to higher or lower elution solvent utilization.

2.2. Optimizing solvent selection for butyric acid desorption from weak-base resins

Minimizing the amount of elution solvent used to recover the target product after the adsorption step is key to reducing the raw material cost and energy demand of WBA. As discussed in the introduction, organic solvents are attractive over aqueous elution systems such as hot water or dilute acids or bases because the organic solvent displaces water during elution and can be recycled within the process (Fig. 1). Here we select several common solvents with the goal to minimize the eluent volume requirement and to maximize the concentrate the target product in the eluent, thereby reducing the volume processed during downstream distillation and resulting in an energy savings. To that end, the adsorption capacity of butyric acid on the resins PVP, PBI, and Dowex 77 were measured in the elution solvents: acetone, methanol, DMSO, Cyanex 923 (CX), and a mixture of 10 wt% Cyanex 923, 90 wt% acetone (CX-acetone). We selected Cyanex 923, a mixture of trialkyl phosphine oxides (the composition is provided in Table S2†), as one of the elution solvents because it is typically used as a volatile fatty acid extractant[19] and thus we hypothesized it to be a strong elution solvent for butyric acid from resins. Measuring the adsorption capacity of the resin in these solvents allows quantification of the ability of the solvent to remove the target product from the resin.

Fig. 3A shows measured data points of the adsorption capacity of butyric acid on PVP in the selected elution solvents. The Dowex 77 and PBI adsorption capacity data in solvents are shown in Fig. S1A and B† respectively. DMSO dissolved the PBI resin during the experiment and therefore this resin–solvent combination is not applicable. All solvent data sets were fit to a variant of the Freundlich model, described by eqn (3) to quantify the desorption constant of the solvents.

$$q = \frac{1}{K_R}\left(C_{EQ}\right)^{n^{-1}}. \quad (3)$$

In eqn (3), q is the adsorption capacity of acid onto the resin (kg acid per kg dry resin), C_{EQ} is the equilibrium concentration of acid remaining in the solvent after uptake (g L^{-1}), K_R is the desorption constant of the solvent and is a constant that is proportional to the preference of the acid for the solvent phase over the resin phase (g L^{-1}), and n^{-1} is a constant that indicates the linearity of the isotherm.

The Freundlich constants K_R and n^{-1} values determined from eqn (3) are listed in Table 2. Since, as shown in Fig. 2B, the adsorption constant (K) trends with a known parameter of the resin (pK_a), we similarly correlate the desorption constant (K_R) with a known parameter of the solvent. In Fig. 3B, we relate the $\log_{10}(K_R)$ to the basicity of the solvent. To represent the basicity of the solvent, the hydrogen-bond acceptor basicity (β(OH)) scale of the solvent was used which is derived from the linear solvation energy relationship developed *via* NMR shifts (Table S3†).[45] The linear relationship between the $\log_{10}(K_R)$ and its basicity (β(OH)) is useful because it quantitatively predicts the desorption constant of a solvent simply by knowing the solvent basicity, information that is readily available for many solvents.[42] Note that the basicity of more complex solvent mixtures such as Cyanex 923 in acetone is not known and therefore this solvent is not plotted within Fig. 2B.

Furthermore, the desorption capacity of the solvents is dependent on the resin used, where the solvent K_R value decreases as the resin K value increases. This relationship is illustrated by the arrow in Fig. 3B. The relationship between K_R and K was then quantified in Fig. 4, where $\log_{10}(K_R)$ is plotted as a function of the β(OH) of the solvent divided by the pK_a of the resin. Fig. 4 shows $\log_{10}(K_R)$ in terms of two well-known parameters, namely the resin pK_a and solvent basicity, thereby enabling prediction of K_R from the resin pK_a and solvent basicity. This result gives a foundation for defining the relationship between the solvent demand needed during elution and the β(OH)/pK_a. This is because K_R can be used to estimate the

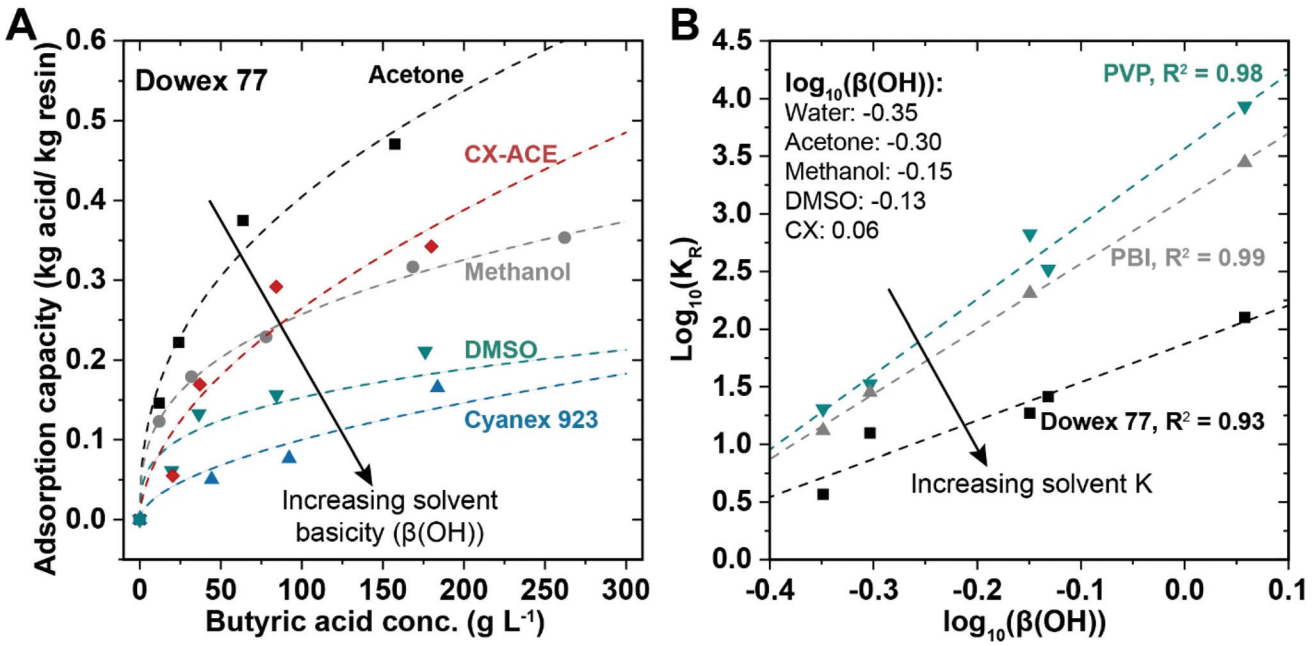

Fig. 3 Equilibrium isotherms in solvents. (A) The experimental equilibrium data points show the adsorption of butyric acid on Dowex 77 in the presence of solvents. The data points are fit (dashed lines) to the Freundlich model (eqn (3)) to determine the desorption constant (K_R) (Table 2) of solvents which is a constant inversely proportional to the affinity of the acid for the resin. (B) The $\log_{10}(K_R)$ is plotted *vs.* the $\log_{10}$ of the basicity (β(OH)) of the solvent and a linear relationship is shown.

Table 2 Eqn (3) Freundlich parameters

Resin	Water	Acetone	Methanol	10 wt% CX in ACE	DMSO	Cyanex 923 (CX)
			K_R			
Dowex 77	3.7	16.3	18.7	47.9	26	126
PBI	13.2	28.3	205.1	n/a	n/a	2790
PVP	20.4	33.4	671	181	330	8580
			n^{-1}			
Dowex 77	0.29	0.30	0.34	0.55	0.30	0.55
PBI	0.53	0.44	0.72	n/a	n/a	1.1
PVP	0.59	0.30	0.83	0.54	0.34	1.3

maximum concentration of butyric acid in the solvent (Fig. 3), which is useful to estimate the minimum solvent demand. In the next section, we quantify this relationship between β(OH)/pK_a and the required solvent volume needed to desorb butyric acid from a fixed-bed column.

2.3. Fixed-bed column demonstration

Butyric acid adsorption and elution was demonstrated using fixed-bed columns to determine the column break-through-point (BTP), the maximum product concentration in the eluate, and the recovery as a function of solvent addition. To generate the breakthrough curve, a solution of 20 g L^{-1} butyric acid was passed over fixed-bed columns of each resin. The outlet concentration (C_{out}) of butyric acid was measured to determine the BTP, which corresponds to the volume at which butyric acid appears in the flow through (Fig. S2†).

After the BTP was determined for each resin, columns of each resin were prepared and loaded to the BTP with butyric acid. To initially screen the fixed-bed system for effective recovery of butyric acid from the resins, acetone was selected as the elution solvent and was fed to the column to elute adsorbed butyric acid. Note that during elution with a solvent such as acetone, the adsorbed acid and interstitial water were removed from the column. The interstitial water is the water that is not adsorbed on the resin but left in the void space (between resin particles and inside the resin pores) of the column during loading. Once the interstitial water was removed, eluted water and butyric acid exited the column together. Fig. 5A shows the butyric acid concentration in the eluate normalized to the butyric acid feed concentration (20 g L^{-1}) and Fig. 5B shows the percent mass recovery of butyric acid in the eluate normalized to the initial mass of butyric acid adsorbed on the column.

In terms of the amount of solvent needed to recover butyric acid, PBI, which was provided in as a non-crosslinked material, requires 2–3× more acetone than PVP and Dowex 77 to reach

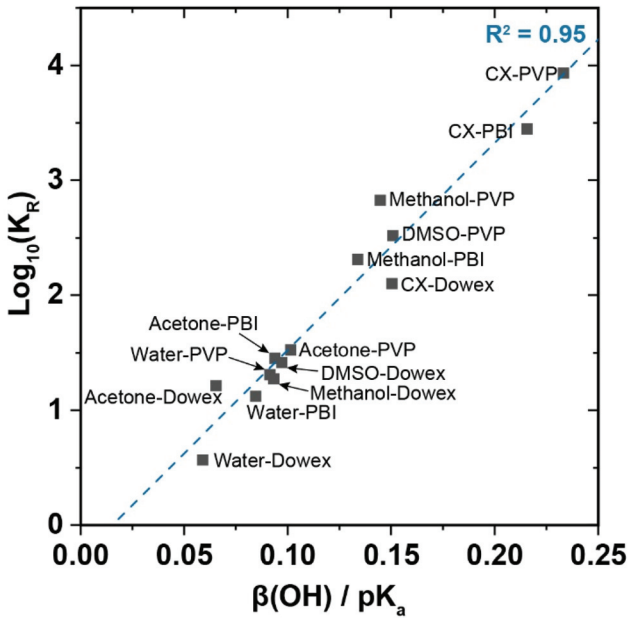

Fig. 4 Estimating K_R. The $\log_{10}(K_R)$, which was determined from fitting equilibrium data (Fig. 3) with the Freundlich isotherm model (eqn (3)), is plotted as a function the β(OH) of the solvent/pK_a of the resin. A liner relationship is shown, enabling prediction of K_R from the β(OH) and the pK_a.

50% butyric acid recovery. This result is explained by the difference in wet density between the resins. PBI resin has a volume of 9 mL g^{-1} of wet PBI, whereas PVP and Dowex 77 each have a wet density of 2.6 mL g^{-1} of wet resin. Therefore, the total PBI interstitial volume including the void space in the resin and void space between resin particles is greater than both PVP and Dowex 77. Accordingly, more acetone is needed to displace the volume in the void space and because of the larger solvent requirement, only PVP and Dowex 77 were considered for further fixed-bed experiments.

Next, additional solvents were used for elution of butyric acid from fixed-bed columns packed with either Dowex 77 or PVP to show the performance of various resin–solvent pairings. Methanol, DMSO, and 10 wt% Cyanex 923 in acetone were chosen as the additional elution solvents. Note that we attempted to use Cyanex 923 as an elution solvent without diluting in acetone, but this attempt led to a two-phase eluate with butyric acid product in both phases, thereby presenting an additional separation challenge. Therefore, Cyanex 923 was diluted in acetone to 10 wt% to form a water miscible solvent (Fig. S3†) to prevent two-phase elution fractions. Dowex 77 and PVP were loaded to their respective BTP and the selected solvents were used to elute butyric acid. For both Dowex 77 and PVP, we show the chromatogram, with a normalized eluate concentration relative to the initial fed concentration of butyric acid (20 g L^{-1}), for elution using methanol (Fig. S4A†), DMSO (Fig. S4C†) and the CX–acetone mixture (Fig. S4E†).

The butyric acid mass recovery (relative to the initial adsorbed mass of butyric acid) upon elution is shown for each resin–solvent combination next to the elution curves (Fig. S4B, S4D and S4F†). We note that 100% mass recovery of butyric acid was achieved with all solvents if PVP or PBI was used; however, during elution of butyric acid from Dowex 77, less

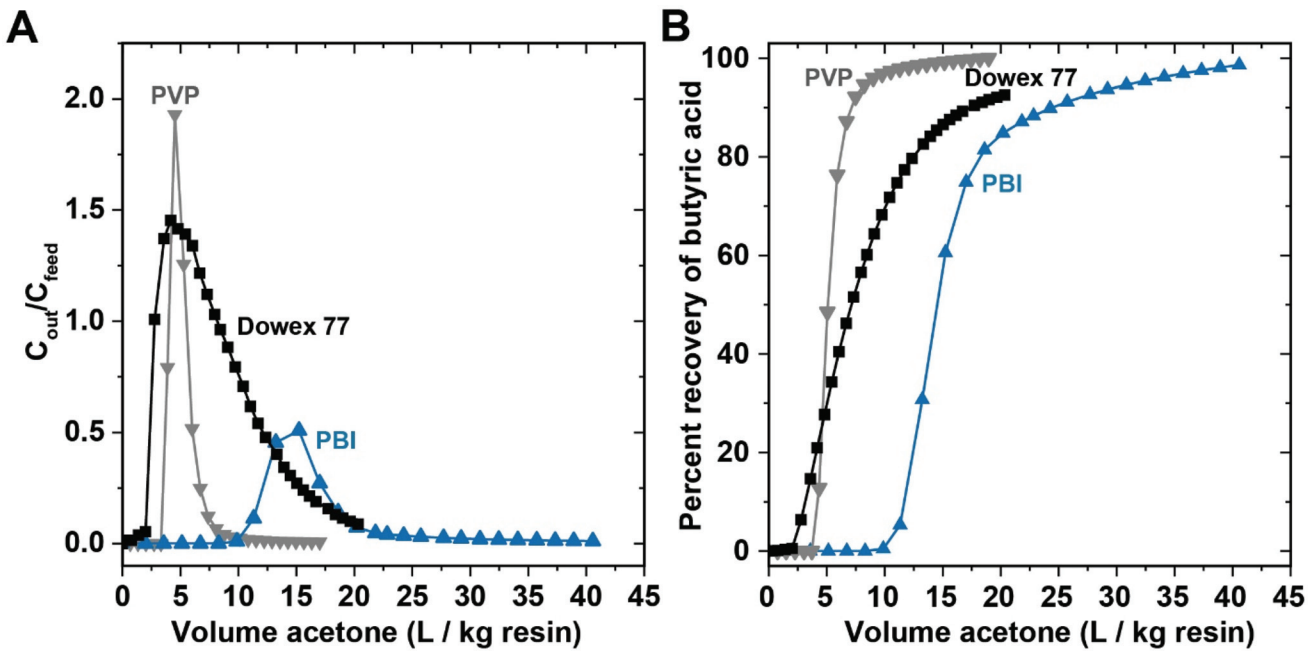

Fig. 5 Elution of butyric acid from fixed-bed columns. (A) Elution profiles of butyric acid from the PVP, PBI, and Dowex 77 resins using acetone as the elution solvent. (B) The percent recovery is the percent of butyric acid collected in the eluate normalized to the initial mass of butyric acid adsorbed to the resin before elution.

than 100% butyric acid was recovered (a maximum of 92% was reached with acetone, 95% with methanol, 91% with DMSO, and 76% with CX–acetone). The incomplete recovery from Dowex 77 is likely due to irreversible binding of butyric acid onto the resin caused by the presence of ionic functional groups such as quaternary amine groups on the resin. Here, the maximum recovery during the first bind-elute cycle is ~95% for Dowex 77. However, if the column is put through multiple bind-elute cycles and the ionic sites remain bound to acid molecules between cycles, the second cycle can achieve 100% recovery since additional acid is not lost to the ionic sites.

Lastly, we determined the solvent demand to achieve 95% butyric acid recovery from fixed-bed columns and plotted these results as a function of the β(OH) of the solvent divided by the pK_a to show the relationship to the solvent demand of the solvent–resin system (Fig. 6). For PVP, the experimental solvent demand was determined at 95% recovery from Fig. 5B, Fig. S4B, and S4D† for acetone, methanol, and DMSO, respectively. Note that we did not use the solvent demand for the CX–acetone mixture in Fig. 6 because the β(OH) of this solvent is unknown and because of the tailing effect seen during elution from Dowex 77 (Fig. S4E†) which may be caused by slow desorption kinetics.[46] For Dowex 77, to account for irreversible binding, the solvent demand was determined at 95% recovery relative to the maximum recovery recorded, which was 95% in methanol (Fig. S4B†). Accordingly, for Dowex 77, the solvent demand was determined from fixed-bed data at the experimental 90% recovery (which is 95% of 95%) and these results are plotted in Fig. 6. For Dowex 77, the experimental solvent demand was determined from Fig. 5B, Fig. S4B, and S4D† for acetone, methanol, and DMSO, respectively. All other solvent–resin combinations were estimated (gray squares in Fig. 6) from the fixed-bed experimental trend (R^2 = 0.96). Note that Fig. 6 gives the solvent demand on the basis of per dry mass of resin. Therefore, to calculate the solvent demand on a per mass of product basis, the fit from Fig. 6 was divided by the adsorption capacity (q) which has units of kg acid per kg resin:

$$S_D = \frac{0.34}{q}\left(\frac{\beta(OH)}{pK_a}\right)^{-1.47} \quad (4)$$

In eqn (4), S_D is the solvent demand (kg solvent per kg butyric acid), β(OH) is the hydrogen-bond acceptor basicity of the solvent, and the pK_a is the apparent pK_a of resin.

The exponential trend between solvent demand and β(OH)/pK_a allows one to estimate the solvent demand in a fixed-bed system for any resin–solvent combination barring experimental challenges such as solvent–water miscibility and tailing effects. Minimizing solvent demand is important because there is an associated downstream distillation energy demand and raw material cost per liter of solvent used as described in the next section on solvent recycling.

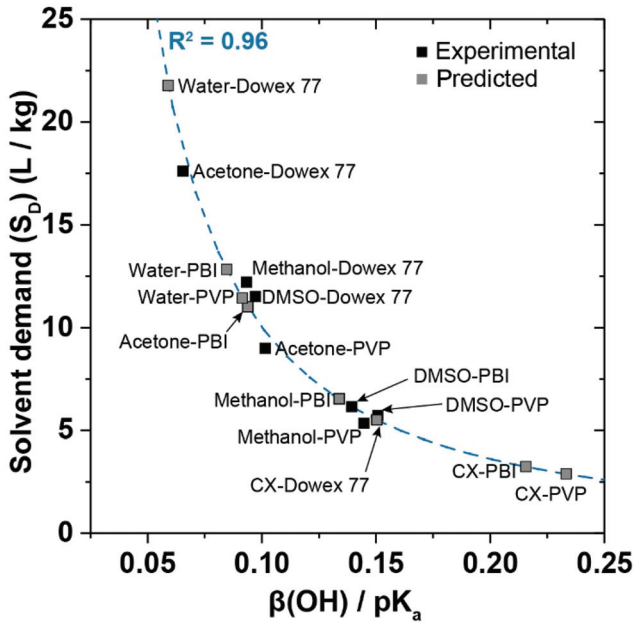

Fig. 6 Solvent demand for butyric acid recovery from fixed-bed columns. The solvent demand (S_D) (L kg^{-1} butyric acid) is plotted *vs.* the β(OH) of the solvent divided by the pK_a of the resin. The experimentally determined data from fixed bed columns (black squares) are fit to an exponential (eqn (4)) to predict the S_D of the other resin–solvent combinations that were not measured (grey squares).

2.4. Solvent recycling and butyric acid isolation *via* distillation

An Aspen Plus process model for solvent recycling and butyric acid isolation downstream of the weak-base adsorption/desorption was constructed (Fig. 7) to estimate the energy consumption and operating costs of the process. In this process model, heat integration, specifically heat exchanger networks (HENs) and mechanical vapor recompression (MVR), was used to reduce distillation energy consumption. Distillation models were developed to isolate butyric acid from the following solvents: acetone, methanol, 10 wt% Cyanex 923 in acetone, and 10 wt. trioctylamine (TOA) in acetone. Note the thermodynamic properties for Cyanex 923 are not in the Aspen Plus database, therefore we used the known physical and chemical properties of Cyanex 923 to create a user-defined component within Aspen Plus. We also included results from TOA which is chemically similar to Cyanex 923 and is defined in the Aspen Plus database. DMSO was not modelled here because of its azeotrope with butyric acid and the autocatalytic decomposition safety hazards associated with DMSO distillation.[47] The results provided below exhibit a similar trend between all of the solvents modelled and, therefore, provide a general correlation for estimating the energy consumption.

The process model for each recovery scenario generally follows Fig. 7. Detailed Process Flow Diagrams (PFDs) of butyric acid and water removal from acetone, methanol, and 10 wt% TOA or Cyanex 923 in acetone are shown in Fig. S5 and S6.† In Fig. 7, the feed stream is the eluate from the fixed-bed column and is initially fed to a flash drum where solvent is vaporized *via* vacuum distillation at 20 °C. This enables much

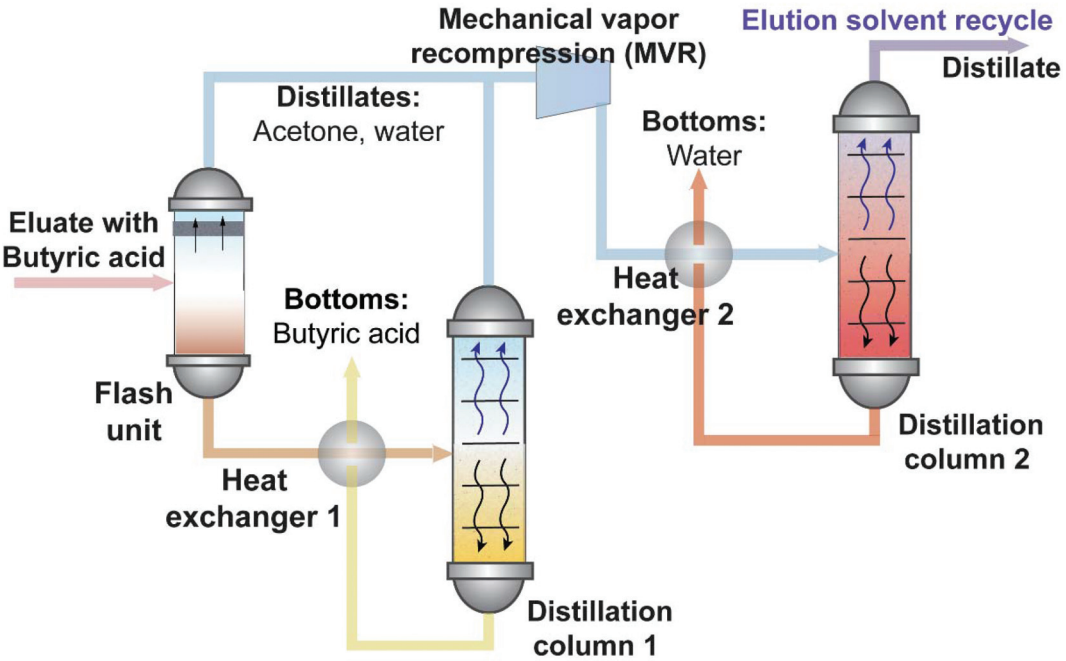

Fig. 7 Process flow diagram (PFD) for butyric acid recovery and solvent recycling. The distillation train to separate butyric acid from the elution solvent involves a flash drum followed by two distillation columns with heat integration strategies including mechanical vapor recompression post column 1 and heat exchangers for stream preheating.

of the solvent to bypass the first multi-stage distillation column, where butyric acid is separated from water and residue solvent. The vaporized solvent from the flash is then compressed to 0.25 atm using mechanical vapor recompression to supply enough heat to power the reboiler of the solvent recovery column. The bottoms from the flash are sent to the butyric acid recovery column. In Fig. 7, there are two HENs present in the distillation train. The first is the integration of the bottoms from the butyric acid recovery column with the feed for the column. The second is the integration of the bottoms from the solvent/water column with recompressed vapor from the compressor. Note that for recovery of butyric acid from 10 wt% TOA or Cyanex 923 in acetone, an additional column is needed before the butyric acid recovery column to recover the heavy solvent (Fig. S6†). Information on the stream composition, temperature, and pressure is given for all systems in Tables S4–S6.†

The distillation model was optimized to minimize the energy footprint of the system while achieving >95% butyric acid recovery, >99 wt% butyric acid purity, and >99% solvent recovery. The distillation feed stream composition was established to represent the eluate stream from a fixed-bed column. The fixed-bed experiments show the feed solution of butyric acid (20 g L^{-1}) can be concentrated in the eluate up to 5-fold (Fig. S4C†). However, the eluate concentration of butyric acid depends on the specific resin–solvent combination and several other operating parameters such as the percent recovery in the eluate and the initial concentration (titer) of butyric acid in the bioprocessing broth before adsorption occurs, which is typically less than 150 g L^{-1}.[2] Therefore, we modelled the distillation process over a wide range of butyric acid concentrations (15–150 g L^{-1}) to show the influence of the butyric acid concentration in the eluate on energy consumption. A concentration of 5 wt% water in the distillation feed stream was assumed to account for the residual water that is carried over from desorption. The water elution profile from the column depends on column operating parameters such as flow rate and product recovery, and ranges from a ~7.6 wt% in our data to below 1 wt% in simulated moving bed (SMB) systems with optimized switching sequences.[22] From an energy footprint perspective, the heat and electrical duty drop exponentially as the concentration of butyric acid increases in the eluent (feed) to distillation train (Fig. S7†). The heating duty is associated with the distillation reboilers. The electrical duty is associated with the pumps and compressor power requirements for each process. The total combined heat and electrical duty is shown in Fig. 8A for each solvent recycling process on a per kg butyric acid basis. The energy consumption of the process is shown in the light of the total energy in the product stream or the heat of combustion of butyric acid (24.8 MJ kg^{-1} butyric acid) and with respect to 20% of the heat of combustion which is a relevant value that was achieved for the case of acetic acid recovery from an LLE process with solvent recovery.[19] A process energy that is less than <20% of the heat of combustion can be achieved at butyric acid concentrations >60 g L^{-1}. By averaging the total distillation duty of the acetone, methanol, and TOA–acetone processes at eight butyric acid concentrations, we found that the total average

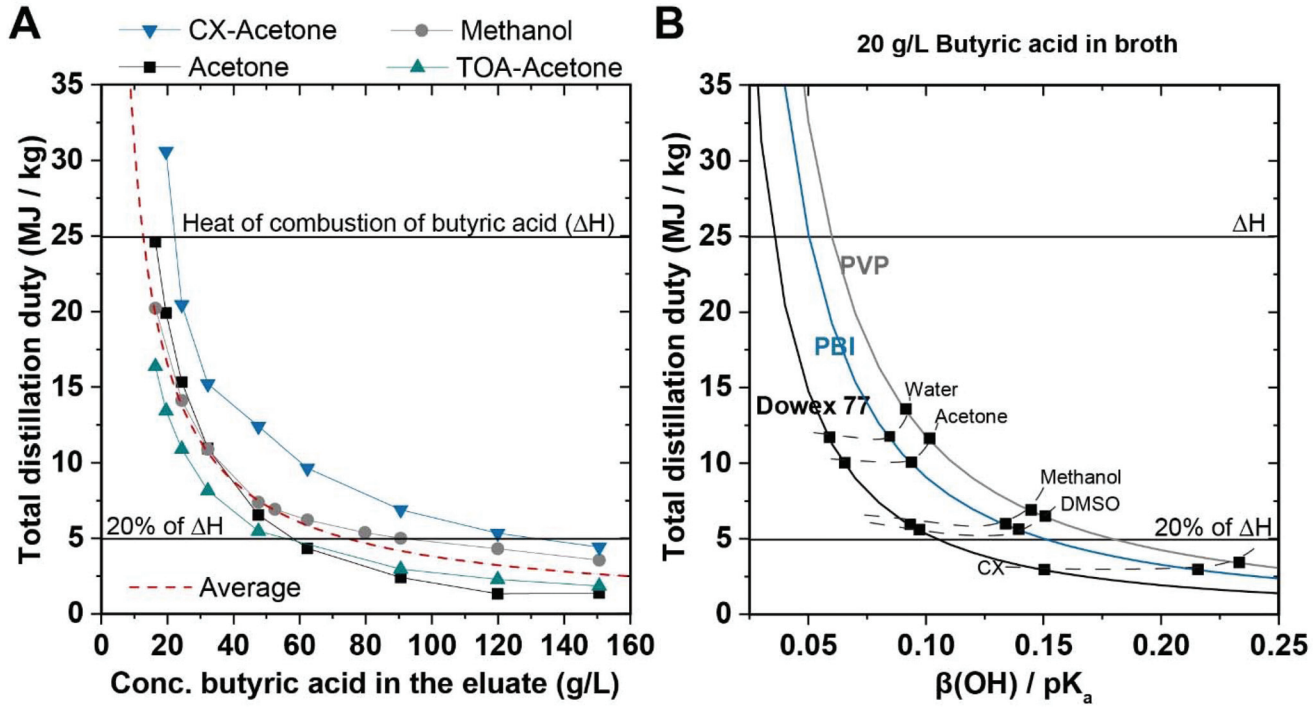

Fig. 8 Total distillation duty. (A) The total distillation duty for solvent recovery processes is shown with the average fit for the total distillation duty. (B) The total distillation duty as a function of the solvent divided by the pK_a of the resin (eqn (6)).

duty is inversely proportional to the concentration of butyric acid in the feed (eqn (5), red dashed line Fig. 8A). Eqn (5) suggests that the total duty depends solely on the distillation feed concentration of butyric acid and is independent of the organic solvent chosen. Eqn (5) was derived from processes that do not include an azeotrope and were optimized *via* heat integration and mechanical vapor recompression technology.

$$E = \frac{0.32}{C_F}. \quad (5)$$

In eqn (5), E is the total distillation duty (MJ kg^{-1} of butyric acid) and C_F is the feed concentration to the distillation process (kg of butyric acid L^{-1}).

To show the energy consumption as a function of the β(OH)/pK_a value of the solvent–resin system, we combined eqn (4) and (5). The two equations can be combined since the distillation feed concentration (C_F) in eqn (5) is the inverse of the solvent demand (L kg^{-1} acid). The energy consumption is then estimated from the β(OH)/pK_a value *via* eqn (6):

$$E = \frac{0.11}{q}\left(\frac{\beta(\mathrm{OH})}{\mathrm{p}K_a}\right)^{-1.47} \quad (6)$$

Results from eqn (6) are shown in Fig. 8B for Dowex 77, PBI, and PVP systems assuming an initial bioprocess concentration of 20 g L^{-1}. As shown by eqn (6) and in Fig. 8B, the total distillation energy requirement depends on the adsorption capacity (q) and the β(OH)/pK_a value. As shown above in eqn (3), the adsorption capacity is a function of the product concentration in the broth and the adsorption constant (K) *via* the Freundlich model. Since the adsorption constant is estimated from the resin pK_a through eqn (S2) or (S3),† the total distillation energy requirement is estimated by knowing the resin pK_a and the solvent β(OH). An example calculation is provided in the discussion section to show this methodology. Lastly, the distillation energy demand has an associated OPEX and environmental impacts as discussed in the following section.

2.5. Techno-economic analysis (TEA) of butyric acid recovery by adsorption technologies

The production costs of carboxylic acids from bioprocessing are traditionally dominated by the cost associated with downstream processing (DSP) due to the equimolar raw material to product requirements of conventional approaches such as precipitation and strong IX.[21] To show the economic benefits of reducing raw material demand, a comparative TEA was performed between the conventional strong IX adsorption approach and WBA processes that offer reduced material demand due to solvent recycling. For each technology, the total operating expense (OPEX) and capital expenditures (CAPEX) were estimated based on a per kg of butyric acid basis. As further described below, the OPEX for the WBA processes was determined as a summation of (1) the resin and solvent raw material cost over the lifetime of the plant (30 years) and (2) the heat and energy cost associated with distillation. For all cases described below, the CAPEX was determined assuming a production capacity of 166 kiloton butyric acid per year, simulating the production capacity of a typical biorefin-

ery for biofuel production (Table S7†).[48] Our initial TEA was based on a bioprocessing titer of 20 g L^{-1} butyric acid; however, the upstream bioprocess titer is dependent on many factors, and accordingly a sensitivity analysis was performed to determine the sensitivity of operating cost to the butyric acid titer (1 to 100 g L^{-1}). Additionally, key economic drivers of the WBA process were identified below, including the percent recovery of the solvent and the cost of the resin. Sensitivity analyses were generated for these economic drivers to show their impact on the OPEX.

We selected the PVP and Dowex 77 resins for the TEA because they provided enhanced performance over PBI in the fixed-bed configuration as shown in Fig. 5A where the peak concentration of butyric acid in the acetone eluate from the PBI resin is lower than the initial concentration ($C_{out}/C_{feed} < 1$) indicating dilution of the product during elution. The bulk raw material resin cost was estimated to be \$15 kg^{-1} for Dowex 77 and \$875 kg^{-1} for PVP (Table S8† shows the cost estimates for resins, solvents and utilities and the discussion section reviews the cost difference between Dowex 77 and PVP). A resin lifetime of 5-years was assumed to be the identical for PVP and Dowex 77 based on industrial data for weak-base resins and accounting for adsorption capacity losses over time.[49] The resin demand, or the mass (kg) of resin needed per mass (kg) of butyric acid in the feed bioprocess broth, for PVP and Dowex 77 was estimated using the adsorption isotherm Freundlich model and parameters (eqn (2) and Table 1). The resin productivity (mass of butyric acid adsorbed per hour per mass of resin) was estimated based on the experimental fixed-bed conditions at a feed flow of 3 bed-volumes per hour and is 6.0 h^{-1} for both Dowex 77 and PVP. The resin cost is \$0.41 kg^{-1} butyric acid for PVP processes and \$0.003 kg^{-1} of butyric acid for Dowex 77 processes (Fig. 9).

The OPEX associated with downstream elution solvent recycling includes (1) the cost of replenishing solvent that is lost from the distillation system, and (2) the heating and electrical duty of the distillation system. Solvent losses are a known economic driver and therefore were considered in our TEA for the WBA processes.[50] In our process model, we found that the elution solvent is primarily lost *via* the wastewater stream (Tables S4–S6†). The solvent recovery was approximately 99 wt% for acetone and methanol, and 99.9 wt% for TOA or Cyanex 923. Note that the TOA and Cyanex 923 solvents are much heavier than water (the normal boiling point of these solvents is >300 °C) and therefore easily separated from water by distillation. For the TEA, we selected elution solvents including water, acetone, methanol, and Cyanex 923. DMSO was not included in the TEA model because of the azeotropic distillation requirement and safety concerns for this solvent as stated in the previous section. Water was included here because hot water has been used previously as an elution solvent (Table S1†) and a distillation process to separate water from butyric acid has also been previously described.[18] The initial solvent change (L solvent per kg resin) into the process was estimated based on the exponential trend in Fig. 6 (eqn (4)). Note that the solvent demand from eqn (4) (L solvent per kg resign) is on a per kg of resin basis and is converted to a per kg acid basis by dividing by the adsorption capacity of the resin (kg butyric acid per kg resin). The solvent costs on a per acid basis are then shown in Fig. 9 for each process.

Lastly, the energy consumption of the distillation process was translated to an operating cost by using the utility price

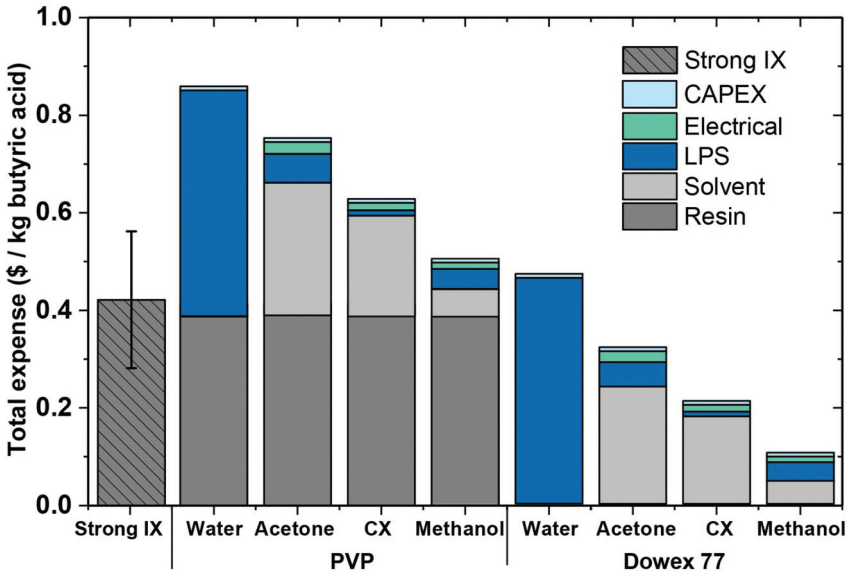

Fig. 9 Total expense of the WBA and strong IX processes. The estimated combined OPEX and CAPEX of weak-base adsorption (WBA) processes are shown on a per kg of butyric acid product. The operating cost estimate includes the resin, solvent, heating, and electrical cost of operating the adsorption and distillation processes to recover 99 wt% butyric acid and ~99% of the process solvent. The estimated expense of the strong IX exchange process is also shown for comparison. LPS: low pressure steam.

(Table S8†) of low-pressure steam (LPS) and electrical power. The heating operating cost is associated with the reboiler duty and the electrical power cost is associated with running compressors to maintain vacuum during distillation. The electrical and heating demand is a function of the butyric acid concentration in the eluate as shown in Fig. S7.† The butyric acid concentration in the eluate is determined as the inverse of the solvent consumption (L solvent per kg resin), which was estimated from Fig. 6. For the WBA processes that use water as an eluate, the distillation process includes azeotropic distillation, estimated to be 81.3 MJ kg^{-1} of butyric acid.[18]

In comparison to strong IX technology, WBA processes generally have a lower OPEX because the WBA process consumes fewer raw materials. The strong IX process for the recovery of carboxylic acids from fermentation broth relies on ionic binding mechanisms to anion exchange resins.[21] That process binds the carboxylate anion to the resin and the elution of the bound carboxylate anion requires a concentrated acid solution such as 4 M hydrochloric acid.[51] Therefore, every mole of butyric acid requires one mole of sodium hydroxide to convert the butyric acid into carboxylate and one mole of hydrochloric acid (HCl) to elute. This process adds substantial raw material OPEX. For every kg of butyric acid, the anion exchange process costs \$0.42 for the sodium hydroxide and \$0.13 for the hydrochloric acid. Accordingly, the total strong ion exchange process is approximately \$0.58 kg^{-1} of butyric acid product when the resin cost, CAPEX, and downstream distillation cost is incorporated. The strong IX process utilizing NaOH/HCl is 5.3-fold more than the cost of the entire Dowex 77-methanol WBA process. However, there are alternative chemicals to HCl and NaOH such as H_2SO_4 that have less of an economic burden. In Fig. 9 we show the average of four strong IX cases utilizing various acids and bases (Table S9†). Furthermore, a separation challenge exists to isolate butyric acid from the aqueous eluate of the anion exchange process. To avoid azeotropic distillation, the butyric acid needs to be eluted from the resin at a concentration above the azeotrope (the azeotrope between butyric acid and water is at 18.4 wt% butyric acid).

A cost sensitivity analysis was also performed highlighting the implications of resin lifetime and solvent percent recovery. Here the impact of resin raw material cost (50–1000 \$ kg^{-1} resin) on OPEX with a process feed stream containing 20 g butyric acid per L for the PVP process is calculated. As shown in Fig. S8A,† the OPEX associated with replenishing the resin is linearly dependent on the resin material cost. To maintain a resin OPEX lower than \$0.25 kg^{-1} butyric acid, the cost of the resin must be less than \$570 kg^{-1} of dry resin. Next, a sensitivity analysis was performed on the percent of solvent recovered within the process. Fig. S8B† shows the sensitivity of acetone, methanol, and Cyanex 923 losses for a process with the PVP resin. To maintain an operating solvent cost that is less than \$0.25 kg^{-1} butyric acid, the solvent losses from the distillation process must be <1.0% for acetone, <4.0% for methanol, and <0.05% for Cyanex 923. Ultimately, the OPEX associated with resin and solvent is a key driver on the total operating cost, highlighting an important consideration in solvent and resin selection.

2.6. Environmental impacts of the WBA process

To assess the environmental impact of the WBA process compared to the conventional strong IX process, two environmental impacts were estimated: greenhouse gas (GHG) emissions and fossil energy demand (FED). The boundary of the environmental impact assessment was limited to the separation process. Additionally, butyric acid is an intermediate for renewable fuel and chemical production and the product use phase and end of life were not considered here. GHG emissions were determined in grams of carbon dioxide equivalent (CO_{2e}) using a 100-year GHG emission factor.[52] FED and GHG emissions of raw materials and utilities are listed in Table S10.† The GHG emissions and FED for the WBA process and IX process are shown in Fig. S9† for PVP and Fig. 10 for Dowex 77. The resin GHG for all processes is <0.003 kg CO_{2e} per kg butyric acid and the FED of the resin is <0.04 MJ kg^{-1} butyric acid. Table S11† lists the GHG emissions for four strong IX cases and Fig. 10A shows the results from the NaOH/HCl approach. Fig. 10B shows that all of the WBA processes utilize less fossil energy than the heat of combustion of butyric acid (24.8 MJ kg^{-1} butyric acid). The strong anion exchange process requires 45.0 MJ of fossil energy per kg of butyric acid due to the energy required to produce the required sodium hydroxide (*via* the electrolytic chloralkali process)[53] and hydrochloric acid. The lowest possible FED demand of strong IX is 17.4 MJ kg^{-1} when sulfuric acid and ammonium hydroxide are employed (Table S12†). However, this lower estimated end is still considerable compared to WBA at 3.7 MJ kg^{-1} of butyric acid as estimated for the Dowex 77 resin with Cyanex 923 as the elution solvent, which is 12.2-fold lower than the NaOH/HCl strong IX process and 14.9% of the heat of combustion of butyric acid.

3. Discussion

The results obtained here lead to the development of a simple methodology for optimizing a WBA process to a lower OPEX, energy demand, and carbon footprint to enable cost-competitive and sustainable production of bio-based carboxylic acids. First, we note that in the literature, several weak-base resin–solvent combinations are suggested for carboxylic acid recovery from aqueous streams; however there is no general framework for selecting combinations that ultimately optimize the material (resin and solvent) demand and lower the energy demand.[31,41] In order to streamline estimating the performance and TEA of any resin–solvent pair, a direct method of estimating the resin, solvent, and energy demand of the WBA process from readily available fundamental properties (solvent basicity and the resin pK_a) and bioprocess parameters (pH and titer) is provided below.

3.1. Resin demand (mass of resin per mass of product)

The resin demand is the inverse of the adsorption capacity (mass product per mass resin) which is estimated from eqn (2), the Freundlich isotherm model. To solve the Freundlich

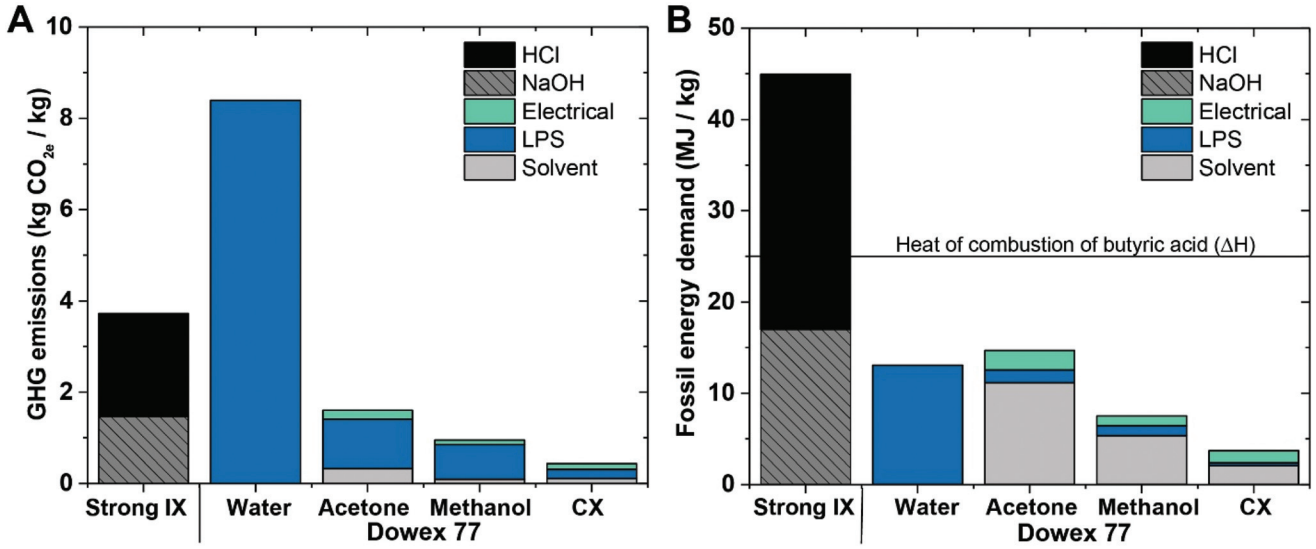

Fig. 10 Environmental impacts. (A) Fossil energy demand and (B) The GHG emission of the WBA processes using the Dowex 77 resin compared with the strong IX process.

isotherm model, the following three input parameters are needed: (1) the pK_a (either the apparent or monomer pK_a) of the resin, (2) the pH of the bioprocess broth, and (3) the titer (total grams of product per volume) of the bioprocess broth.

The apparent pK_a of the resin is a commonly available parameter listed from the manufacture. However, if the resin apparent pK_a is not listed, the functional group or active site monomer pK_a can be used to calculate the resin demand. With knowledge of the apparent or functional group pK_a one can determine the Freundlich isotherm parameters (K and n) used in eqn (2) which are needed to solve for the adsorption capacity. The K parameter is the adsorption constant and is calculated *via* eqn (S2)† (uses the functional group pK_a) or (S3)† (uses the resin apparent pK_a). The n parameter in eqn (2) also correlates to the pK_a and is calculated *via* eqn (S4)† (uses function group pK_a) or eqn (S5)† (uses the apparent pK_a).

The pH and titer of the bioprocess broth are required to estimate the resin demand. Specifically, an ideal bioprocess broth would have a pH below the pK_a of the acid and sufficient titer to provide a driving force to adsorb protonated acids onto the resin functional groups. When the pH of the broth is below the pK_a of the acid (the pK_a of butyric acid is 4.82), a majority of the butyric acid is in the protonated (free) state and can bind to the weak-base resin through a hydrogen bonding mechanism. However, when the broth pH is above the pK_a of the acid, a majority of the acid is in the unprotonated butyrate form (the negatively charged carboxylate form) resulting in an absence of a driving force between the carboxylate and the uncharged weak-base resin. The ratio between the free acid concentration [HA] and carboxylate concentration [A^-] in the bioprocess broth is estimated by the Henderson–Hasselbalch equation (eqn (S6)†). Since there are two unknowns in the Henderson–Hasselbalch equation ([HA] and [A^-]), a mole balance (eqn (S7)†) is needed to specify the system. Note that the mole balance sets the known titer equal to the summation of the [HA] and [A^-] where each term is multiplied by the broth volume in order to give units of moles. Thereby, the input parameters, pH, and titer of the upstream bioprocess, are needed to solve for the free acid concentration in the broth.

Once the Freundlich parameters (K and n) and the free acid concentration are estimated as described above, eqn (2) is used to estimate the adsorption capacity (q). The inverse of the adsorption capacity (q) is the resin demand (mass resin per mass product).

3.2. Solvent demand (volume solvent per mass of product)

The solvent demand is the amount of solvent needed per mass of product to desorb 95% of the product from the resin in a fixed-bed configuration. The solvent demand is estimated from the adsorption capacity and the β(OH)/pK_a value *via* eqn (4). The β(OH) for many elution solvents is reported in the literature and is experimentally determined by NMR spectroscopy.[42] The adsorption capacity is determined using the methodology presented in the resin demand section above and is a function of the titer, pH, and resin pK_a.

3.3. Energy demand (energy per mass of product)

The total distillation energy demand of the solvent recycling process is the energy required to achieve a 95% butyric acid recovery, 99 wt% butyric acid purity, and 99% solvent recovery. The energy demand is calculated by eqn (6) with input parameters including the known adsorption capacity (q) and the β(OH)/pK_a value. We derived eqn (6) from the solvent demand equation (eqn (4)) and the energy–concentration relationship (eqn (5)) to estimate the energy demand *via* the adsorption capacity (q) and the β(OH)/pK_a value.

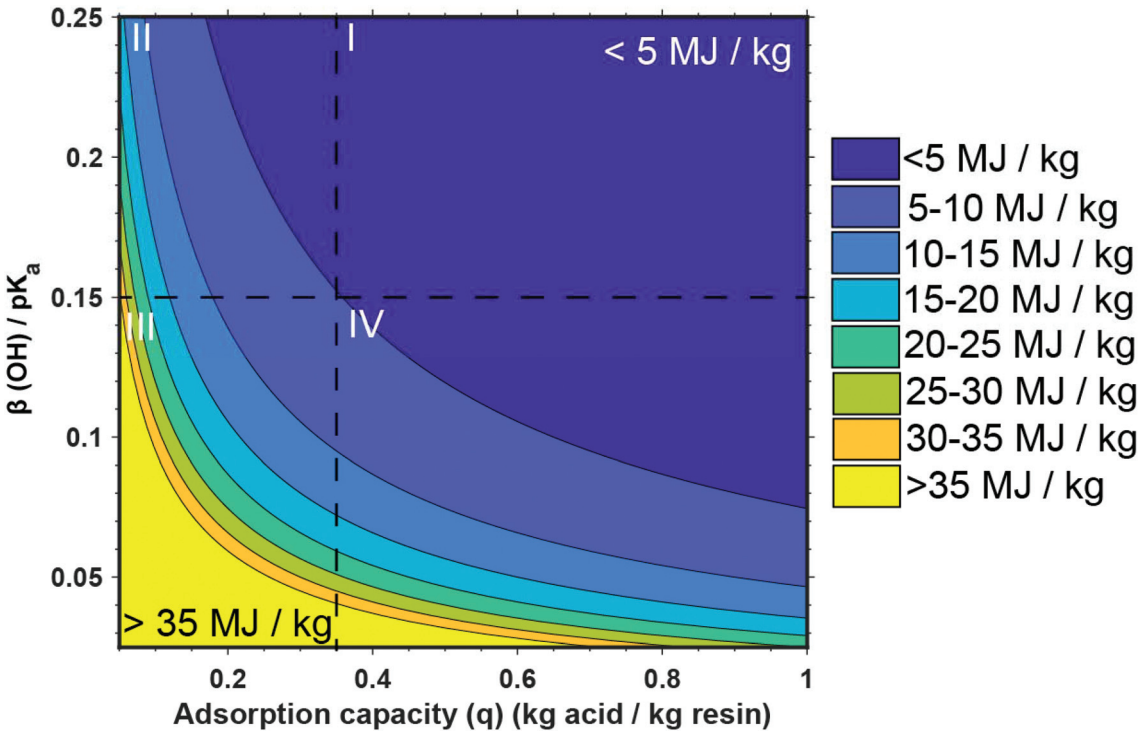

Fig. 11 Energy demand as a function of the adsorption capacity (q) and the solvent β(OH)/resin pK_a value. The contour plot (each contour is 5 MJ kg^{-1}) shows the q and β(OH)/pK_a range where the system is optimized from an energy demand balance (within the dark blue area). The WBA process has the least energy input at high q (>0.35) and at high β(OH)/pK_a (>0.15) as shown by quadrant I. In the dark blue region, the energy requirement asymptotically approaches ~1 MJ kg^{-1} and the total energy input is below 5 MJ kg^{-1} or 20% of the butyric acid heat of combustion (24.9 MJ kg^{-1}).

As detailed above, the input variables required to estimate process demands (resin, solvent, and energy demand) are the solvent basicity (β(OH)) and the adsorption capacity (q) which is a function of the titer, pH, and resin pK_a. To show the impact of q and the β(OH)/pK_a value on the total distillation energy demand, we provide a contour plot generated by solving eqn (6) (Fig. 11). The change in energy demand between contour lines is 5 MJ kg^{-1}. The dark blue region has an energy demand between 1–5 MJ kg^{-1} (the energy requirement asymptotically approaches ~1 MJ kg^{-1}). We note that many of our solvent–resin combinations have a β(OH)/pK_a value in the range of 0.05–0.2 (Fig. 6). At the high end of this range (β(OH)/pK_a value >0.15), the minimum q value needed to achieve <5 MJ kg^{-1} is 0.35 (quadrant I in Fig. 11). At lower β(OH)/pK_a values, a q > 0.35 is needed to maintain the <5 MJ kg^{-1} region as indicated by quadrant IV. However, if q for the process is low (<0.35), a high β(OH)/pK_a value (>0.15) is needed to access low energy demand (<5 MJ kg^{-1}) zone as shown in quadrant II. In quadrant III (low q and low β(OH)/pK_a), the energy demand rapidly increases as the β(OH)/pK_a value decreases below 0.15 and as the q value decreases below 0.35. In order to operate in the low energy zone (dark blue region), a q value >0.35 is generally needed. A high q value can be achieved in two ways: (1) changing upstream bioprocess conditions (pH and titer) or (2) increasing the pK_a of the resin. However, if the pK_a of the resin is increased, the β(OH)/pK_a value decreases, and accordingly, a higher β(OH) or q is necessary to off-set the change.

Given that DSP costs for fermentation derived chemicals generally contribute 20–40% of the production cost, development of new separation processes should, ideally, fall on the low end of this range.[14] Using the current selling price of butyric acid (~\$1.80 kg^{-1} butyric acid[54]), the DSP target is then \$0.36 (20% of \$1.8) kg^{-1} of butyric acid. We show in Fig. 9 that the total DSP expense for several WBA processes fall below this target including the acetone–Dowex 77 process (\$0.32 kg^{-1}), the CX–Dowex 77 process (\$0.20 kg^{-1}), and the methanol–Dowex 77 process (\$0.11 kg^{-1} which is 6% of the current selling price of butyric acid). These results are promising, since the conventional IX approach leads to a total expense of \$0.58 kg^{-1} (5.3-fold more than the methanol–Dowex 77 process). However, the total DSP expense is influenced by several variables that are not linked to the performance of the WBA process including the (1) cost of the resin, (2) cost of the solvent, and (3) the cost of utilities such as LPS and electricity. For the resins, the difference in cost between materials may be the result of the differing synthesis and end-use. For example, PVP resin is primarily used for nuclear applications and is composed of a relatively expensive weak-base monomer, 4-vinylpyridine, synthesized to make up the entire resin material.[55,56] However, Dowex 77 has a high-volume use in the sugar purification processes and is made up of the commodity

plastic polystyrene which is then functionalized with a tertiary amine,[57] leading to a lower cost ($15 kg^{-1}) as compared to PVP ($875 kg^{-1}) (Table S8†).

The WBA process performance is negatively affected by fermentation streams that contain components that compete for adsorption sites on the resin. For example, during an auxiliary recovery process downstream of the primary recovery process (*e.g.*, a WBA process downstream of precipitation is an example of an auxiliary process) ions such as sulfates can interfere with carboxylic acid binding to tertiary amine functionalized resins such as Dowex 77, therefore lowering the adsorption capacity.[23] To avoid unnecessary loss of adsorption capacity, pretreatment processes such as microfiltration, nanofiltration, ion exchange, and activated carbon adsorption may be necessary before adsorption to improve the capacity of the resin.[20,30] If glucose is not removed before WBA, glucose isotherms are available in the literature for adsorption on PVP and tertiary amine weak base resins that can be used to estimate reductions in adsorption capacity due to competitive binding.[58] In addition, multiple acid products may compete for binding sites. The adsorption of several acids onto the resin can be predicted using the pure component isotherms in a multi-component adsorption model developed previously.[59]

Mixed solvents have been suggested in the literature for carboxylic acid recovery from weak-base resins, including the Cyanex 923/acetone mixture developed here, and trimethylamine (TMA)/methylisobutylketone (MIBK) mixture used for lactic acid elution.[41] Mixed solvent systems may offer performance advantages such as decreased solvent demand due to the use of a 'strong' solvent with a high basicity, however, water miscibility (Fig. S3†) are recommended for fixed-bed adsorption systems to prevent the product from partitioning between organic and aqueous phase in the elute. Furthermore, solvents with high basicity such as Cyanex 923, are typically more expensive than common solvents such as methanol and acetone (Table S8†). Also, for TMA systems, López-Garzón and Straathof[21] note that the use of TMA as a solvent is difficult to use because of its strong odor and the energy requirements needed to break the TMA-acid complex. Instead, common solvents may provide the best balance between performance and OPEX, with the tradeoff being their basicity range may be more limited.

4. Conclusion

Adsorption technology is an effective and widely used method to separate bioproducts including carboxylic acids,[21] proteins,[60] natural products,[61] pharmaceuticals,[62] and environmental pollutants such as heavy metals,[63] phosphorus,[64] and perfluoroalkyl substances (PFAS)[65] from aqueous streams. Weak-base resins are an emerging class of materials for carboxylic acids recovery, enabling elution of the product with common solvent recovery and solvent recycling, therefore leading to both economic and environmental advantages compared to the conventional strong IX approach. The optimized WBA process has a 5.3-fold lower cost compared with the strong IX process and reduced the FED by up to 12.2-fold. Additionally, we developed a methodology to estimate the raw material and energy demand of the process based on fundamental resin and solvent properties, namely the pK_a of the resin and basicity of the solvent as well as process parameters including the pH and titer of the bioprocess broth. The WBA process has an energy input less than 20% of the heat of combustion of butyric acid at high q (>0.35) and a high $\beta(OH)/pK_a$ (>0.15). These results encompass a guide to optimize WBA processes in terms of performance, economic feasibility, and environmental impacts for the recovery of bio-based carboxylic acids.

5. Experimental

5.1. Resin selection and preparation

PVP (Vertellus, IN) (18–50 mesh), PBI (PBI Performance, NC) (>30 mesh), and Dowex 77 (Dow, MI) (29–36 mesh) are macroreticular resins that were chosen over similar gel-type resins because macroreticular resins are highly stable, crosslinked, porous structures that often have longer lifetimes than microporous resins.[49,66] Resins were washed in 5 mL of 4 wt% NaOH (aq) per gram of resin for 2 hours, vacuum filtered to drain NaOH, flushed with deionized water until the effluent was pH neutral, and then washed with 10 mL of methanol per gram of resin. The resins were then dried to constant weight in a vacuum oven (21 mm Hg, 49 °C) and stored in a desiccator until use. Dowex 77 is currently sold under the trade name AmberLite FPA77 UPS by DuPont (Wilmington, DE). Amberlite IRA-96, which has the same functional group, backbone, and adsorption constant as Dowex 77 is also currently available through DuPont and was prepared to validate the Dowex 77 isotherm behavior (data not shown).

5.2. Adsorption isotherms

0.1 grams of resin was added to 4 mL of a butyric acid solution (0, 1, 5, 10, 20, 50, 80 or 100 g L^{-1} butyric acid) in an Amicon Ultra-4 10 kDa regenerated cellulose concentrator (prepared according to the specification of manufacture). Samples were incubated on a rotary shaker for at least 24 hours (kinetics are shown in Fig. S10†). To remove the interstitial water, the samples were centrifuged at 4000*g* in a swinging bucket rotor for 30 min. The flow through was weighed and sampled to determine the uptake of butyric acid. To determine the adsorption capacity of butyric acid in elution solvents (acetone, methanol, DMSO, Cyanex 923, 10 wt% Cyanex 923 in acetone), 0.5 grams of resin was added to 4 grams of elution solvent. The sample was incubated for 24 hours and the liquid was sampled by LC.

5.3. Liquid chromatography and refractive index detection

Analysis of samples was performed using an Agilent 1200 LC system (Agilent Technologies, Santa Clara, CA) equipped with a G1362A refractive index detector (RID). Each sample and

standard were injected at a volume of 20 μL onto a BioRad Aminex HPX-87H column 9 μm, 7.8 × 300 mm column (BioRad, Hercules, CA) with a RID and column temperature of 55 °C. Compounds were separated utilizing an isocratic flow of 0.01 N H_2SO_4 in water at 0.6 mL min^{-1} for a total run time of 52 min. Standards were purchased from Sigma Aldrich (Sigma Aldrich, St Louis, MO). The concentrations of the calibration curve ranged from 0.05 g L^{-1} to 50 g L^{-1}. A minimum of 5 calibration concentrations was used with an r^2 coefficient of 0.995 or better for each analyte and a check calibration standard (CCS) was analyzed every 10 samples to ensure the integrity of the initial calibration.

5.4. Breakthrough and elution curves

A GE XK 16/20 (16 mm ID, 200 mm maximum bed height) column was packed with 5 grams of resin, using a flow rate of 10 mL min^{-1} (deionized water). The columns were then loaded to the breakthrough point with a 20 g L^{-1} butyric acid solution at a flow rate of 3 bed volumes per hour (Cole-Parmer single head piston pump).[31] After loading, the elution solvent was used to remove the interstitial water and elute adsorbed water and butyric acid. Eluent fractions were analyzed by liquid chromatography and Karl Fischer. A photo of the column set-up is provided in the ESI (Fig. S11†).

5.5. Karl Fischer titration

Karl Fischer (KF) titrations were conducted with a 701KF Titrino unit, using CombiTitrant 5 (Merck, Kenilworth, NJ) titrant. Calibration of titrant was performed before any sample analysis, using 1% water in 1-methoxy-2-propanol standard (Merck). Samples were added directly to anhydrous methanol (KF samples containing acetone were added to Combisolvent keto solvent (Millipore Sigma)) in the titration cell for KF moisture determination. The sample aliquot was ~0.1 g, each aliquot was weighed before titration.

5.6. Aspen plus process model

See ESI† for information on the thermodynamic parameters utilized.

5.7. Freundlich model

The Freundlich parameters were fit to the experimental data using a Trust-Region-Reflective non-linear fitting algorithm in MATLAB.

5.8. Techno-economic analysis (TEA)

TEA determined butyric acid separation cost butyric acid solutions for each resin and solvent combination scenario. Aspen Plus process models that incorporated experimental data were developed to solve mass and energy balances for each unit operation. The material and energy flows from the process models allow for the estimation of the associated capital and operating costs. The equipment costs were estimated based on the scale of 21 075 kg h^{-1} of butyric acid yield that is consistent with the NREL's 2018 biochemical design report.[48] Table S8† shows the summary of the butyric acid separation cost attributed to the capital expenditures. The operating costs were estimated for the integrated separation design based on the material and energy inputs and the unit prices shown in Table S10.†

5.9. Environmental impact

GHG emissions are represented in grams of carbon dioxide equivalent (CO_{2e}) using a 100-year GHG emission factor.[52] Fossil energy demand is determined based on the method published by Ecoinvent version 2.0[67] and expanded by PRé Consultants for raw materials available in the SimaPro 7 database.[68] The input inventories that captures the impacts of input raw materials and energy provide the necessary information required to perform the LCA modeling to quantify greenhouse gas (GHG) emissions and fossil energy consumption. We used the DATASMART Life Cycle Inventory Package[69] which is a dataset representative of the North American region provided containing expanded modified Ecoinvent processes[67] to reflect U.S. conditions and the U.S. LCI processes (USLCI) to account for embodied emissions and energy flows. The GHG and FED basis values for electricity and heating (natural gas) are applied consistently with the values utilized in GREET 2016. The factors are used to convert the life-cycle inventory to the partial life cycle GHG emissions and fossil energy demand, which are expressed in CO_{2e} and megajoule (MJ) per kg of product, respectively.

Conflicts of interest

P. S., E. M. K., L. M., and H. M. are inventors on a patent application submitted by the Alliance for Sustainable Energy on Advanced Adsorption Processes for Bio-derived Products (U.S. Patent App. No. 16/942,888 filed on July 30, 2020).

Acknowledgements

The research reported in this paper was sponsored by the U.S. Department of Energy (DOE), Energy Efficiency and Renewable Energy Office, Bioenergy Technologies Office (BETO) under the BETO Bioprocessing Separations Consortium *via* Contract No. DE-AC36-08GO28308 with the National Renewable Energy Laboratory. The authors gratefully acknowledge the support of Nichole Fitzgerald and Gayle Bentley at BETO. We thank Laura Hollingsworth for critically reviewing the manuscript. The views expressed in the article do not necessarily represent the views of the U.S. Department of Energy or the U.S. Government. The U.S. Government retains and the publisher, by accepting the article for publication, acknowledges that the U.S. Government retains a nonexclusive, paid-up, irrevocable, worldwide license to publish or reproduce the published form of this work, or allow others to do so, for U.S. Government purposes.

References

1 B. Erickson and P. Winters, *Biotechnol. J.*, 2012, **7**, 176–185.
2 A. J. Straathof, *Chem. Rev.*, 2014, **114**, 1871–1908.
3 M. T. Agler, B. A. Wrenn, S. H. Zinder and L. T. Angenent, *Trends Biotechnol.*, 2011, **29**, 70–78.
4 S. P. Chundawat, G. T. Beckham, M. E. Himmel and B. E. Dale, *Annu. Rev. Chem. Biomol. Eng.*, 2011, **2**, 121–145.
5 J. Xu, J. Hao, J. J. Guzman, C. M. Spirito, L. A. Harroff and L. T. Angenent, *Joule*, 2019, **3**, 885–888.
6 A. M. Henstra, J. Sipma, A. Rinzema and A. J. Stams, *Curr. Opin. Biotechnol.*, 2007, **18**, 200–206.
7 X. Huo, N. A. Huq, J. Stunkel, N. S. Cleveland, A. K. Starace, A. E. Settle, A. M. York, R. S. Nelson, D. G. Brandner, L. Fouts, P. C. St. John, E. D. Christensen, J. Luecke, J. H. Mack, C. S. McEnally, P. A. Cherry, L. D. Pfefferle, T. J. Strathmann, D. Salvachúa, S. Kim, R. L. McCormick, G. T. Beckham and D. R. Vardon, *Green Chem.*, 2019, **21**, 5813–5827.
8 T. J. Schwartz, B. H. Shanks and J. A. Dumesic, *Curr. Opin. Biotechnol.*, 2016, **38**, 54–62.
9 E. Jamalzade, K. Kashkooli, L. Griffin, G. P. van Walsum and T. J. Schwartz, *React. Chem. Eng.*, 2021, **6**, 845–857.
10 N. A. Rorrer, J. R. Dorgan, D. R. Vardon, C. R. Martinez, Y. Yang and G. T. Beckham, *ACS Sustainable Chem. Eng.*, 2016, **4**, 6867–6876.
11 E. M. Karp, T. R. Eaton, V. S. I. Nogué, V. Vorotnikov, M. J. Biddy, E. C. Tan, D. G. Brandner, R. M. Cywar, R. Liu, L. P. Manker, W. E. Michener, M. Gilhespy, Z. Skoufa, M. J. Watson, S. O. Fruchey, D. R. Vardon, R. T. Gill, A. D. Bratis and G. T. Beckham, *Science*, 2017, **358**, 1307–1310.
12 C. R. Soccol, L. P. Vandenberghe, C. Rodrigues and A. Pandey, *Food Technol. Biotechnol.*, 2006, **44**, 141–149.
13 A. Cukalovic and C. V. Stevens, *Biofuels, Bioprod. Biorefin.*, 2008, **2**, 505–529.
14 A. Straathof, *Compr. Biotechnol.*, 2011, **2**, 811–814.
15 J. P. Lange, *Biofuels, Bioproducts and Biorefining: Innovation for a sustainable economy*, 2007, vol. 1, pp. 39–48.
16 G. Centi and R. A. van Santen, *Catalysis for renewables: from feedstock to energy production*, John Wiley & Sons, 2008.
17 A. A. Kiss, J.-P. Lange, B. Schuur, D. W. F. Brilman, A. G. van der Ham and S. R. Kersten, *Biomass Bioenergy*, 2016, **95**, 296–309.
18 A. M. Lopez and J. A. Hestekin, *Sep. Purif. Technol.*, 2013, **116**, 162–169.
19 P. O. Saboe, L. P. Manker, W. E. Michener, D. J. Peterson, D. G. Brandner, S. P. Deutch, M. Kumar, R. M. Cywar, G. T. Beckham and E. M. Karp, *Green Chem.*, 2018, **20**, 1791–1804.
20 B. Xiong, T. L. Richard and M. Kumar, *J. Membr. Sci.*, 2015, **489**, 275–283.
21 C. S. López-Garzón and A. J. Straathof, *Biotechnol. Adv.*, 2014, **32**, 873–904.
22 J. A. Delgado, V. I. Águeda, M. Á. Uguina, Á. García, J. Matarredona and R. Moral, *Sep. Purif. Technol.*, 2018, **200**, 307–317.
23 M. Van den Bergh, B. Van de Voorde and D. De Vos, *ChemSusChem*, 2017, **10**, 4864–4871.
24 J. Wu, Q. Peng, W. Arlt and M. Minceva, *J. Chromatogr. A*, 2009, **1216**, 8793–8805.
25 M. J. Biddy, R. Davis, D. Humbird, L. Tao, N. Dowe, M. T. Guarnieri, J. G. Linger, E. M. Karp, D. Salvachúa, D. R. Vardon and G. T. Beckham, *ACS Sustainable Chem. Eng.*, 2016, **4**, 3196–3211.
26 DuPont, 2020.
27 S. Kulprathipanja, US4720579A, 1988.
28 L. A. Tung and C. J. King, *Ind. Eng. Chem. Res.*, 1994, **33**, 3217–3223.
29 A. A. Garcia and C. J. King, *Ind. Eng. Chem. Res.*, 1989, **28**, 204–212.
30 E. M. Karp, R. M. Cywar, L. P. Manker, P. O. Saboe, C. T. Nimlos, D. Salvachúa, X. Wang, B. A. Black, M. L. Reed, W. E. Michener, N. A. Rorrer and G. T. Beckham, *ACS Sustainable Chem. Eng.*, 2018, **6**, 15273–15283.
31 N. Kawabata and K. Ohira, *Environ. Sci. Technol.*, 1979, **13**, 1396–1402.
32 C. A. R. Efe, L. A. van der Wielen and A. J. Straathof, *Ind. Eng. Chem. Res.*, 2010, **49**, 1837–1843.
33 G. N. Baroi, I. V. Skiadas, P. Westermann and H. N. Gavala, *AMB Express*, 2015, **5**, 67.
34 C. National Center for Biotechnology Information. PubChem Database. Pyridine, https://pubchem.ncbi.nlm.nih.gov/compound/Pyridine (accessed on Mar. 11, 2020).
35 C. National Center for Biotechnology Information. PubChem Database. Benzimidazole, https://pubchem.ncbi.nlm.nih.gov/compound/Benzimidazole (accessed on Mar. 11, 2020).
36 FooDB, https://foodb.ca/compounds/FDB012648 (accessed Mar. 11, 2020).
37 K. Y. Foo and B. H. Hameed, *Chem. Eng. J.*, 2010, **156**, 2–10.
38 S. M. Husson and C. J. King, *Ind. Eng. Chem. Res.*, 1999, **38**, 502–511.
39 P. Podkościelny and K. Nieszporek, *J. Colloid Interface Sci.*, 2011, **354**, 282–291.
40 W. Rudzinski and W. Plazinski, *J. Colloid Interface Sci.*, 2008, **327**, 36–43.
41 S. M. Husson and C. J. King, *Ind. Eng. Chem. Res.*, 1998, **37**, 2996–3005.
42 C. Laurence and J.-F. Gal, *Lewis basicity and affinity scales: data and measurement*, John Wiley & Sons, 2009.
43 K.-U. Goss and R. P. Schwarzenbach, *Environ. Sci. Technol.*, 2001, **35**, 1–9.
44 M. H. Abraham and F. Martins, *J. Pharm. Sci.*, 2004, **93**, 1508–1523.
45 M. J. Kamlet and R. Taft, *J. Am. Chem. Soc.*, 1976, **98**, 377–383.
46 T. Fornstedt, G. Zhong and G. Guiochon, *J. Chromatogr., A*, 1996, **741**, 1–12.
47 Y. Deguchi, M. Kono, Y. Koizumi, Y.-I. Izato and A. Miyake, *Org. Process Res. Dev.*, 2020, **24**, 1614–1620.
48 R. E. Davis, N. J. Grundl, L. Tao, M. J. Biddy, E. C. Tan, G. T. Beckham, D. Humbird, D. N. Thompson and

M. S. Roni, *Process Design and Economics for the Conversion of Lignocellulosic Biomass to Hydrocarbon Fuels and Coproducts: 2018 Biochemical Design Case Update; Biochemical Deconstruction and Conversion of Biomass to Fuels and Products via Integrated Biorefinery Pathways*, National Renewable Energy Lab.(NREL), Golden, CO (United States), 2018.

49 DuPont, 2019.

50 V. H. Shah, V. Pham, P. Larsen, S. Biswas and T. Frank, *Ind. Eng. Chem. Res.*, 2016, **55**, 1731–1739.

51 A. V. Sosa, P. R. Córdoba and N. I. Perotti, *Biotechnol. Prog.*, 2001, **17**, 1079–1083.

52 T. F. Stocker, D. Qin, G.-K. Plattner, M. Tignor, S. K. Allen, J. Boschung, A. Nauels, Y. Xia, V. Bex and P. M. Midgley, *Contribution of working group I to the fifth assessment report of the intergovernmental panel on climate change*, 2013, p. 1535.

53 J. Crook and A. Mousavi, *Environ. Forensics*, 2016, **17**, 211–217.

54 L. Jiang, H. Fu, H. K. Yang, W. Xu, J. Wang and S.-T. Yang, *Biotechnol. Adv.*, 2018, **36**, 2101–2117.

55 K. Takahashi, S. Miyamori, H. Uyama and S. Kobayashi, *Macromol. Rapid Commun.*, 1997, **18**, 471–475.

56 J. G. Kennemur, *Macromolecules*, 2019, **52**, 1354–1370.

57 D. C. Sherrington, *ChemComm*, 1998, 2275–2286.

58 Y. Dai and C. J. King, *Ind. Eng. Chem. Res.*, 1996, **35**, 1215–1224.

59 S. M. Husson and C. J. King, *Ind. Eng. Chem. Res.*, 1999, **38**, 502–511.

60 D. Stanic, J. Radosavljevic, M. Stojadinovic and T. C. Velickovic, in *Ion Exchange Technology II*, Springer, 2012, pp. 35–63.

61 F. Bucar, A. Wube and M. Schmid, *Nat. Prod. Rep.*, 2013, **30**, 525–545.

62 D. P. Elder, *J. Chem. Educ.*, 2005, **82**, 575.

63 M. V. Mier, R. L. Callejas, R. Gehr, B. E. J. Cisneros and P. J. Alvarez, *Water Res.*, 2001, **35**, 373–378.

64 A. Bottini and L. Rizzo, *Sep. Sci. Technol.*, 2012, **47**, 613–620.

65 F. Dixit, B. Barbeau, S. G. Mostafavi and M. Mohseni, *Environ. Sci.: Water Res. Technol.*, 2019, **5**, 1782–1795.

66 D. T. Gjerde and J. S. Fritz, *Ion chromatography*, Interbook, 1987.

67 R. Frischknecht, N. Jungbluth, H.-J. Althaus, G. Doka, R. Dones, T. Heck, S. Hellweg, R. Hischier, T. Nemecek, G. Rebitzer and M. Spielmann, *Int. J. Life Cycle Assess.*, 2005, **10**, 3–9.

68 R. Frischknecht, N. Jungbluth, H.-J. Althaus, C. Bauer, G. Doka, R. Dones, R. Hischier, T. Nemecek, A. Primas and G. Wernet, The Swiss Centre for Life Cycle Inventories (ecoinvent), 2007, pp. 1–40.

69 D. P. Dupuis, R. G. Grim, E. Nelson, E. C. Tan, D. A. Ruddy, S. Hernandez, T. Westover, J. E. Hensley and D. Carpenter, *Appl. Energy*, 2019, **241**, 25–33.

